

A USAXS Study of the Morphology of High-pressure Crystallized Ultrahigh-molecular-weight Polyethylene

M. Turell, A. Bellare

Department of Orthopedic Surgery, Brigham and Women's Hospital, Harvard Medical School, Boston, MA, U.S.A.

Introduction

Ultrahigh-molecular-weight polyethylene (UHMWPE) is used worldwide as a bearing material in orthopedic implant devices. The problem of wear debris generated by the articulation of UHMWPE components against metallic implant counterfaces continues to be a major problem limiting the lifespan of joint prosthetics [1, 2]. UHMWPE is manufactured by processes such as compression molding and ram extrusion that apply elevated temperatures and pressures to the UHMWPE resin powder. The resulting bulk material usually has a crystallinity of 50-55%. It is well known that the degree of crystallinity has a strong influence on several mechanical properties such as Young's modulus, ultimate tensile properties, and resistance to fatigue crack propagation [3, 4]. In this study, the crystalline morphology resulting from high-pressure crystallization was quantitatively characterized by using ultrasmall-angle x-ray scattering (USAXS) at the UNI-CAT beamline of the APS, low-voltage scanning electron microscopy (LVSEM), and differential scanning calorimetry (DSC). The series of crystallization temperatures used in these experiments was chosen to encompass a range of temperatures above and below the orthorhombic to hexagonal crystal transition temperature for polyethylene at an applied pressure of 500 MPa.

Methods and Materials

GUR 1050 (Hoechst-Ticona, Bayport, TX) UHMWPE powder was used as the starting material for all crystallization experiments. The viscosity average molecular weight (M_v) for this resin is estimated to be 5.5 to 6.0×10^6 g/mol on the basis of intrinsic viscosity measurements [7]. Commercial GUR 1050 ram-extruded UHMWPE rod stock (PolyHi Solidur, Ft. Wayne, IN) was used as a control. A high-pressure cell with a cylindrical cavity that was 12.5 mm in diameter was constructed by using D2 tool steel. The cell was first loaded with 3 g of UHMWPE powder and then heated to one of five temperatures (240, 220, 200, 180, or 160°C) at atmospheric pressure by using cartridge heaters controlled by a temperature controller. These temperatures are well above the melting temperature of the UHMWPE powder ($T_m = 141^\circ\text{C}$) at atmospheric pressure, measured by using DSC. These temperatures were maintained for 1 h to allow for complete equilibration before 500 MPa of pressure was applied to the cell by using a Carver

hydraulic laboratory press. The samples were allowed to crystallize for 1 h at 500 MPa and thereafter slowly cooled to room temperature at 500 MPa. Finally, the pressure was reduced to atmospheric pressures. USAXS was performed on 2-mm-thick specimens by using 10-keV x-rays. The beam had a cross-sectional area of 2×0.6 mm. DSC was performed on 4-mg samples by using a Perkin Elmer Pyris 7 instrument. Two DSC passes were performed for each UHMWPE sample. Percent crystallinity was calculated by normalizing the heat of fusion of each sample to the heat of fusion of polyethylene crystal (293 J/g). Crystallinity was taken to be the average of a minimum of three measurements for each group. A JEOL 6320FV LVSEM operating at 2 kV and a working distance of 4 mm were used to image permanganic-acid-etched [6] fracture surfaces of all UHMWPE samples.

Results

USAXS scattering curves were obtained by plotting the scattered intensity (I) vs. q where:

$$q = (4\pi/\lambda)\sin\theta, \quad (1)$$

where θ = one-half of the scattering angle and λ = the wavelength of x-rays (Fig. 1). The USAXS curves revealed a linear Porod region at ultralow q values, suggesting the presence of large-micrometer-size scatterers, such as voids, in all samples, regardless of thermal history. In addition, a broad peak was present in the SAXS region because of scattering from the lamellar morphology.

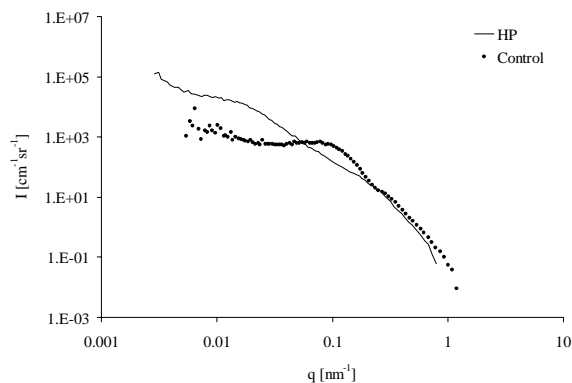


FIG. 1. Scattering plot for high-pressure crystallized and control UHMWPE.

Void scattering was subtracted from scattering curves and replotted as Lorentz corrected intensity to determine the long period or interlamellar spacing (Fig. 2).

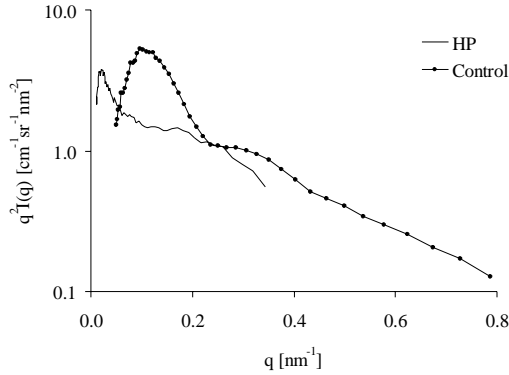


FIG. 2. Plot of $q^2 I$ vs. q for high-pressure crystallized and control UHMWPE.

Because of the presence of broad peaks, it was necessary to obtain long periods from paired distance distribution functions (PDDFs) or $p(r)$ that were identical to the 1-D correlation function for lamellar systems. The scattering functions were converted to PDDFs by using the computer program ITP developed by Glatter [8]. PDDF is related to the scattering function $I(q)$ by the following equation:

$$p(r) = (1/2 \pi^2 A) \int_0^\infty q^2 I(q) \cos(qr) dq, \quad (2)$$

where $p(r)$ = the paired distance distribution function, A = the area of the lamella, $I(q)$ = the experimental scattering function, q = the scattering vector, and r = the radial distance perpendicular to lamellar surfaces within a stack of lamellae. The USAXS long period for all samples was measured from the peaks present in $p(r)$ (Fig. 3).

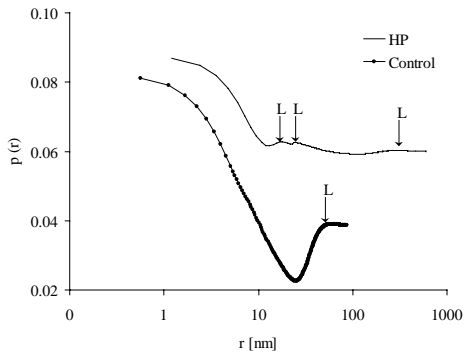


FIG. 3. Paired distance distribution functions $p(r)$. Values of $p(r)$ have been offset for clarity, and values for r are plotted on a log scale.

Together, the long period and DSC crystallinity were used to calculate the lamellar thickness by using the following equation:

$$D = X_c L, \quad (3)$$

where D = the lamellar thickness, X_c = the degree of crystallinity (%) measured by DSC, and L = the USAXS long period (interlamellar spacing). The thickness of the amorphous regions A was also calculated by taking the difference between the interlamellar spacing and the lamellar thickness (Table 1).

Table 1. USAXS characterization of crystalline morphology of high-pressure crystallized and control UHMWPE samples.

Treatment	X_c (%) (DSC)	L (nm) (USAXS)	D (nm)	A (nm)
HP Peak 1	70.0	18.0	12.6	5.4
HP Peak 2	70.0	24.0	16.8	7.2
HP Peak 3	70.0	290.4	203.3	87.1
Control	48.3	65.2	31.5	33.7

DSC thermographs revealed an increase in the melting temperature and overall degree of crystallinity for all high-pressure crystallized UHMWPE samples as compared to control UHMWPE (Fig. 4). Both melting temperature and crystallinity increased steadily in accordance with crystallization temperature and reached maximum values at a crystallization temperature of 220°C (Table 2).

Table 2. DSC results for high-pressure crystallized and control UHMWPE. TC = crystallization temperature, TM = melting temperature, XC = % crystallinity ($\pm 3\%$)

TC (°C)	TM (°C) Pass I	TM (°C) Pass II	XC (%) Pass I	XC (%) Pass II
Control	136.2	132.4	57.8	48.0
160	144.3	133.0	78.1	48.0
180	145.2	131.7	82.8	47.7
200	146.4	131.9	86.6	48.1
220	147.0	131.7	90.7	48.2
240	146.4	131.7	91.1	45.7

The crystallinity of the commercial UHMWPE sample was approximately 10% higher than the crystallinity of the

samples slow-cooled under atmospheric temperatures. At 500 MPa, the samples had substantially higher crystallinity than the commercial control UHMWPE, and they increased monotonically with crystallization temperature up to 220°C, whereupon the crystallinity leveled off at approximately 90%. The higher melting temperatures of these samples compared to the control UHMWPE samples indicated the presence of thick crystallites in all samples crystallized at 500 MPa.

LVSEM micrographs of high-pressure and control permanganic-acid-etched fracture surfaces revealed that high-pressure crystallized UHMWPE samples were composed of visibly thicker lamellae compared to control samples (Fig. 4).

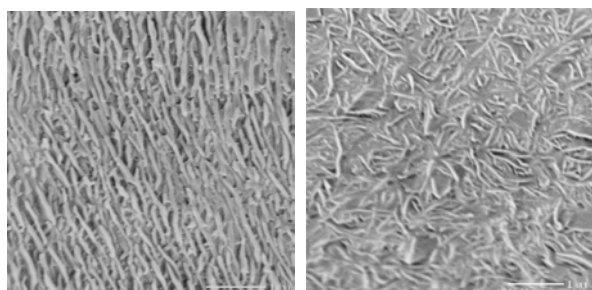


FIG. 4. Low-voltage scanning electron micrograph of lamellar morphology of permanganic-acid-etched fracture surface of high-pressure UHMWPE (left) and control (right). Scale bar = 1 μm .

Discussion

This study revealed that the crystalline morphology of high-pressure crystallized UHMWPE can be elucidated by using USAXS. It is difficult to measure the large interlamellar spacings of UHMWPE by using conventional SAXS, especially for high-pressure crystallized UHMWPE, which has lamellae of 100- to 300-nm thickness. The large range of scattering angles of the USAXS camera of the UNI-CAT beamline enables the morphology of UHMWPE to be measured at both micrometer-length scale (voids) and nanometer-length scale (lamellae). USAXS revealed the presence of voids in bulk UHMWPE due to incomplete consolidation of the

resin powder during processing. The high degree of crystallinity of 80-90% in high-pressure crystallized UHMWPE suggests that large-scale disentanglement of chains occurred to enable chains to be incorporated into lamellae. The samples with higher crystallinity were also associated with higher melting temperatures, indicating that the additional crystallinity was associated with lamellar thickening. The relationship between degree of crystallinity and tribological properties has not yet been fully established. Our long-term goals are to investigate the wear performance and resistance to creep and fatigue properties of these high-crystallinity UHMWPEs and to establish structure-property relationships that govern their corresponding tribological and mechanical behavior.

Acknowledgments

We thank Dr. P. Jemian and Dr. J. Ilavsky for their expert assistance with USAXS measurements. The UNI-CAT facility at the APS is supported by the University of Illinois at Urbana-Champaign, Materials Research Laboratory (U.S. Department of Energy [DOE], State of Illinois-IBHE-HECA, and National Science Foundation), Oak Ridge National Laboratory (DOE), National Institute of Standards and Technology (U.S. Department of Commerce), and UOP LLC. The APS is supported by the DOE Office of Science, Office of Basic Energy Sciences, under Contract No. W-31-109-ENG-38. Additionally, we thank Professor R. E. Cohen at the Department of Chemical Engineering, Massachusetts Institute of Technology, for his guidance in the design and fabrication of the high-pressure cell.

References

- [1] G. Lewis, *J. Biomed. Mater. Res.* **38**, 55-75 (1997).
- [2] I. C. Clarke et al., *Hip Arthroplasty* (Churchill Livingstone, New York, NY, 1991).
- [3] R. W. Truss et al., *Polym. Eng. Sci.* **20**, 747-755 (1980).
- [4] D. Baker et al., *Trans. Soc. Biomat.* **21**, 122 (1998).
- [5] D. C. Bassett et al., *Polym.* **17**, 284-290 (1976).
- [6] R. H. Olley and D. C. Bassett, *Polym.* **23**, 1707-1710 (1982).
- [7] S. M. Kurtz et al., *Biomater.* **20**, 1659-1688 (1999).
- [8] Glatter, *Acta Physica Austriaca* **47**, 83-102 (1977).